Check for updates

Geophysical Research Letters

RESEARCH LETTER
10.1029/2026GL124605

Dust Pollution Mitigation by Solar Farm Deployment in Northern China

Yueting Hao[1,2], Yawen Liu[2], Xin Huang[1,2], Yue Qin[3,4], Rong Tang[3,4], Minghuai Wang[1,2], and Aijun Ding[1,2,5]

[1]State Key Laboratory of Severe Weather Meteorological Science and Technology, Nanjing University, Nanjing, China, [2]Joint International Research Laboratory of Atmospheric and Earth System Sciences, School of Atmospheric Sciences, Nanjing University, Nanjing, China, [3]College of Environmental Sciences and Engineering, Peking University, Beijing, China, [4]Institute of Carbon Neutrality, Peking University, Beijing, China, [5]Nanjing-Helsinki Institute in Atmospheric and Earth System Sciences, Nanjing University, Suzhou, China

Key Points:

- A new model is developed to study how solar farms alter land surface features and local weather conditions to influence dust
- Large-scale solar farms lower air pollution by cutting dust emissions at the source and limiting transport
- Integrating solar farms into desert regions offers a synergistic solution for clean energy and dust pollution control under climate goals

Supporting Information:

Supporting Information may be found in the online version of this article.

Correspondence to:

X. Huang,
xinhuang@nju.edu.cn

Citation:

Hao, Y., Liu, Y., Huang, X., Qin, Y., Tang, R., Wang, M., & Ding, A. (2026). Dust pollution mitigation by solar farm deployment in northern China. *Geophysical Research Letters*, *53*, e2026GL124605. https://doi.org/10.1029/2026GL124605

Received 28 MAY 2026
Accepted 22 AUG 2026

Author Contributions:

Conceptualization: Yueting Hao, Xin Huang, Yue Qin, Aijun Ding
Data curation: Yueting Hao
Formal analysis: Yueting Hao, Yawen Liu
Funding acquisition: Xin Huang, Aijun Ding
Investigation: Yueting Hao
Methodology: Yueting Hao
Project administration: Xin Huang, Aijun Ding
Resources: Yueting Hao
Software: Yueting Hao

© 2026 The Author(s). Geophysical Research Letters published by Wiley Periodicals LLC on behalf of American Geophysical Union.
This is an open access article under the terms of the Creative Commons Attribution-NonCommercial License, which permits use, distribution and reproduction in any medium, provided the original work is properly cited and is not used for commercial purposes.

Abstract Dust storms pose a growing threat to air quality and public health across northern China. As part of the carbon-neutrality and clean-air strategy, China is rapidly expanding solar farms, particularly in desert regions, yet their potential to mitigate dust pollution and improve downwind air quality remains poorly understood. Here, we develop an integrated modeling framework to quantify the effects of solar farms on dust emissions, atmospheric transport, and particulate matter pollution in northern China. We find that existing solar farms reduce particulate matter pollution by up to ~5.7 μg/m^3, with reductions reaching approximately 15.9 μg/m^3 (13.8%) under future expansion aligned with China's 2060 carbon-neutrality target. These findings reveal an underappreciated air quality co-benefit of renewable energy infrastructure, underscoring solar farms as a promising dual-purpose strategy for both dust mitigation and decarbonization.

Plain Language Summary Dust storms severely threaten air quality and public health in northern China. China is rapidly expanding large solar farms in desert regions to achieve its 2060 carbon-neutrality goals. However, whether these deployments can also help reduce dust pollution has remained unclear. By using a comprehensive modeling approach, our study reveals that solar panels act as a protective shield on the ground. By covering the landscape, the panels reduce wind speed at the surface and stabilize the soil, making it harder for dust to be lifted into the air. They alter the desert environment and local weather patterns, successfully reducing air pollution. We show that existing solar farms are already contributing to cleaner air, and this positive impact would become much stronger under China's future green energy expansion goals for 2060, which could cut regional air pollution by nearly 14%. This study reveals an underappreciated air quality co-benefit of renewable energy infrastructure, showing its dual benefits for dust mitigation and rapid decarbonization.

1. Introduction

Dust storms, generated when strong winds mobilize erodible soils in arid and semi-arid regions with sparse vegetation, emit up to 2 billion tons of dust into the atmosphere each year (Wu et al., 2022; Zhang et al., 2023). These storm events release large amounts of particulate matter (PM), exerting substantial impacts on global climate and posing serious threats to atmospheric environments, ecosystems, and human health (Kok et al., 2023; Min et al., 2009; Yang et al., 2017). Particularly, dust storms severely degrade air quality in Northern China, where dust from the Gobi Desert is frequently transported downwind into megacities like Beijing (Yang et al., 2022).

To mitigate dust storms, many countries have implemented land-based interventions such as grassland restoration and afforestation (Jiang et al., 2019; Tan & Li, 2015). More recently, large-scale deployment of solar farms in dust-source regions has been increasingly discussed as a potential dust-mitigation measure. Ecological construction around solar farms, for example, artificial planting, can enhance local vegetation cover (Chen et al., 2025; Wang et al., 2024), while dark, dense photovoltaic (PV) panels modify land–atmosphere interactions by reducing surface albedo and increasing aerodynamic roughness (Chang et al., 2020; Stern et al., 2023; Wei et al., 2024). These changes alter the surface energy balance and atmospheric circulation, potentially influencing cloud cover, precipitation, and regional climate through land–atmosphere feedbacks (Chang et al., 2023; Hu et al., 2015; Li et al., 2018; Long et al., 2024; Nguyen et al., 2017; Power et al., 2023). Among these, processes

Supervision: Yawen Liu, Xin Huang, Yue Qin, Aijun Ding
Validation: Yueting Hao
Visualization: Yueting Hao
Writing – original draft: Yueting Hao
Writing – review & editing: Yueting Hao, Yawen Liu, Xin Huang, Yue Qin, Rong Tang, Minghuai Wang

including weakened surface winds, increased precipitation, and vegetation recovery are expected to suppress dust emissions.

Despite these potential effects, the role of solar farms in regulating dust activity has not been quantitatively assessed. Notably, existing PV modeling studies often assume either implausibly large solar farm deployments (Li et al., 2018; Long et al., 2024; Lu et al., 2021) or employ oversimplified albedo treatments (Li et al., 2025; Wei et al., 2024). These simplifications obscure the scale-dependent nature of PV-driven climate responses and limit the applicability of results to real-world solar expansion. Moreover, existing PV schemes typically capture only radiative and aerodynamic adjustments induced by PV arrays, while PV-related ecological pathways, notably vegetation change and soil erosion that directly regulate dust emissions, are largely omitted (Chang et al., 2023; Li et al., 2018). Consequently, the absence of a unified framework that jointly incorporates realistic PV layouts, complete ecological-radiative-aerodynamic pathways, and interactive dust evolution has so far obscured the role of PV deployment in dust mitigation, both mechanistically and quantitatively.

China is at the forefront of combating both severe dust storms and global warming. Driven by ambitious climate goals, China has rapidly expanded its photovoltaic capacity over the past decade, with a large share clustered around the Gobi Desert, a major dust-source region (China Daily, 2023). The ongoing PV expansion provides a natural testbed for evaluating potential dust-mitigation co-benefits of renewable-energy infrastructure. In this study, we systematically investigate solar farms' influence on dust dynamics and quantify their mitigation effects on urban air quality across northern China by integrating multi-source satellite observations with a regional climate–chemistry model featuring a new solar farm parameterization within the GOCART dust emission scheme. This framework characterizes current dust pollution patterns, evaluates PV-induced modifications to land–atmosphere properties, and precisely quantifies resulting reductions in dust emissions, transport fluxes, and urban particulate concentrations. Furthermore, we project future scale-dependent air quality benefits under China's 2060 carbon neutrality pathway. Our results highlight how renewable-energy infrastructure may deliver substantial co-benefits for urban air quality and public health while advancing the clean-energy transition.

2. Materials and Methods

2.1. Impact Assessment of Solar Farms on Surface Properties

We quantify the impacts of solar infrastructure on land surface properties by comparing parameter changes before and after construction. Spatial configuration and construction timelines for solar farms are obtained from Zhang et al. (2022) and Kruitwagen et al. (2021), respectively (see Text S1 and Figure S1 in Supporting Information S1 for data set details). For each solar farm, we employ high-resolution remote sensing data sets to assess its influence on albedo, green vegetation fraction (GVF), and land surface erodibility (EROD). The surface albedo data are obtained from the MODIS Level-3 Version 6.1 MCD43A3 product, which has a 500 m spatial resolution and a daily temporal resolution (Schaaf & Wang, 2021). The GVF is calculated based on satellite-derived Normalized Difference Vegetation Index (NDVI) values (Gutman & Ignatov, 1998). EROD represents the fraction of an erodible grid cell and indicates the probability of sediment accumulation within that cell. It is influenced by topography, vegetation cover, and snow cover (Hao et al., 2024). Detailed formulations for these variables are also provided in Text S1 in Supporting Information S1.

We select 17 solar farms with an area larger than 1 km^2 around the Gobi Desert, each of which has been in operation for more than three years. The affected area of solar farms is defined as the solar farm itself plus a 1-km buffer zone surrounding it (Figure S1 in Supporting Information S1), consistent with previous studies (Xu et al., 2024; Zhang & Xu, 2020). Our analysis evaluates land surface property shifts by calculating the absolute and relative differences between two distinct 3-year windows before and after construction, with specific mathematical formulations detailed in Text S2 in Supporting Information S1.

2.2. Parametrization of Solar Farms' Impact on Land Surface Properties

The construction of large-scale solar farms directly alters key surface properties, including albedo, surface roughness, vegetation cover, and land surface erodibility. The surface parameters for baseline deserts and solar farms are summarized in Table S1 in Supporting Information S1. The model accounts for the effective albedo of solar panels by considering both direct reflectivity and energy conversion efficiency (Li et al., 2018). We estimate the solar farm albedo at approximately 0.34, which represents an absolute reduction of 0.04 relative to the baseline

19448007, 2026, 17, Downloaded from https://agupubs.onlinelibrary.wiley.com/doi/10.1029/2026GL124605 by Xin Huang - Nanjing University , Wiley Online Library on [17/09/2026]. See the Terms and Conditions (https://onlinelibrary.wiley.com/terms-and-conditions) on Wiley Online Library for rules of use; OA articles are governed by the applicable Creative Commons License

19448007, 2026, 17, Downloaded from https://agupubs.onlinelibrary.wiley.com/doi/10.1029/2026GL124605 by Xin Huang - Nanjing University , Wiley Online Library on [17/09/2026]. See the Terms and Conditions (https://onlinelibrary.wiley.com/terms-and-conditions) on Wiley Online Library for rules of use; OA articles are governed by the applicable Creative Commons License

desert value. To reflect the increased aerodynamic resistance caused by the physical structure of the PV arrays, the surface roughness length increases to 0.08 m (Jiang et al., 2021). Furthermore, the parameterization incorporates local vegetation enhancement based on a prescribed 20% relative increase in NDVI compared with the baseline desert (Li et al., 2024; Xia et al., 2023). This updated NDVI subsequently determines the corresponding increase in green vegetation fraction and the decrease in land surface erodibility within the solar farm domains (see Text S3 in Supporting Information S1 for detailed mathematical formulations and derivations).

2.3. Regional Air Quality Modeling and Experimental Scenario Design

This study integrates the new solar farm parameterization into the meteorology–chemistry coupled WRF-Chem model (version 4.4.1) with the GOCART dust emission scheme to evaluate solar farm impacts on atmospheric dust dynamics. The model domain covers the Gobi Desert and northern China, with a horizontal resolution of 20 km and 30 vertical layers extending from the surface to 50 hPa, featuring finer resolution in the lower troposphere to better capture near-surface processes. Simulations are conducted in 96-hr cycles with 24-hr spin up time, using previous outputs as initial conditions for the next run. Physics and chemistry configurations for all simulations are detailed in Table S2 in Supporting Information S1, and for the specific dust emission scheme, please refer to Text S4 in Supporting Information S1.

Numerical experiments consist of sensitivity tests comparing simulations with solar farms against a baseline scenario without solar farms across both present-day and future periods (Table S3 in Supporting Information S1). The present-day scenario incorporates 42 existing solar farms, represented by 33 unique model grid cells with a total area of 13,200 km^2 surrounding the Gobi Desert. The future scenario aligns with China's 2060 carbon neutrality target, expanding the PV deployment area to approximately 140,000 km^2 based on projected solar energy requirements (Qin et al., 2024; Tong et al., 2020). Comprehensive documentation regarding the experimental design is provided in Text S5 in Supporting Information S1. By analyzing these sensitivity experiments, we elucidate the core mechanisms through which solar deployment modulates dust dynamics and simultaneously quantify its mitigation efficacy on regional dust emissions, transport fluxes, and urban particulate matter concentrations.

2.4. Meteorological and Air Quality Observations

To analyze the spatiotemporal variations of dust pollution in northern China, we utilize dust storm records, dust aerosol optical thickness (DAOD), and PM concentration and emission data. Dust storm records are obtained from the National Oceanic and Atmospheric Administration in the Integrated Surface Database (ISD) from the National Oceanic and Atmospheric Administration (NOAA) (Smith et al., 2011). Dust events are identified by weather codes 06, 07, 09, and 30–35, and any occurrence within a day is classified as a dust day. Dust optical depth data (2013–2018) used in this study are obtained from Voss and Evan (2020), a global 1° × 1° data set derived from MODIS measurements. Ground observations of PM_{10} and $PM_{2.5}$ (particulate matter with diameters less than 10 and 2.5 μm) are from China's Ministry of Ecology and Environment. The data on anthropogenic emissions of $PM_{2.5}$ and PM_{10} also came from MEIC for the spring seasons from 2013 to 2020 (Geng et al., 2024; Li et al., 2017), while the anthropogenic emissions of PM_{coarse} (particulate matter with diameters from 2.5 to 10 μm) are also calculated as the difference between PM_{10} and $PM_{2.5}$.

3. Results

3.1. Dust Pollution in Northern China and Solar Farms' Impacts

In spring, intense northwesterly winds mobilize vast volumes of soil dust and transport them eastward and southeastward, degrading air quality across northern China (Figure 1a). Forward trajectory analyses confirm dominant transport pathways from the Gobi Desert into 10 severely affected provinces, which consistently exhibit high dust optical depth and frequent dust days (Figures 1a and 1b; Figure S2 in Supporting Information S1). The mass ratio of PM_{coarse} to PM_{10} serves as a diagnostic indicator of dust pollution, where values exceeding 50% signal dust-dominated conditions (Zhao et al., 2019). As illustrated in Figure 1b, in cities adjacent to the Gobi, such as Hohhot, Lanzhou, and Yinchuan, springtime PM_{coarse}/PM_{10} ratios frequently exceed 60%, underscoring the dominant contribution of desert dust to urban PM pollution.

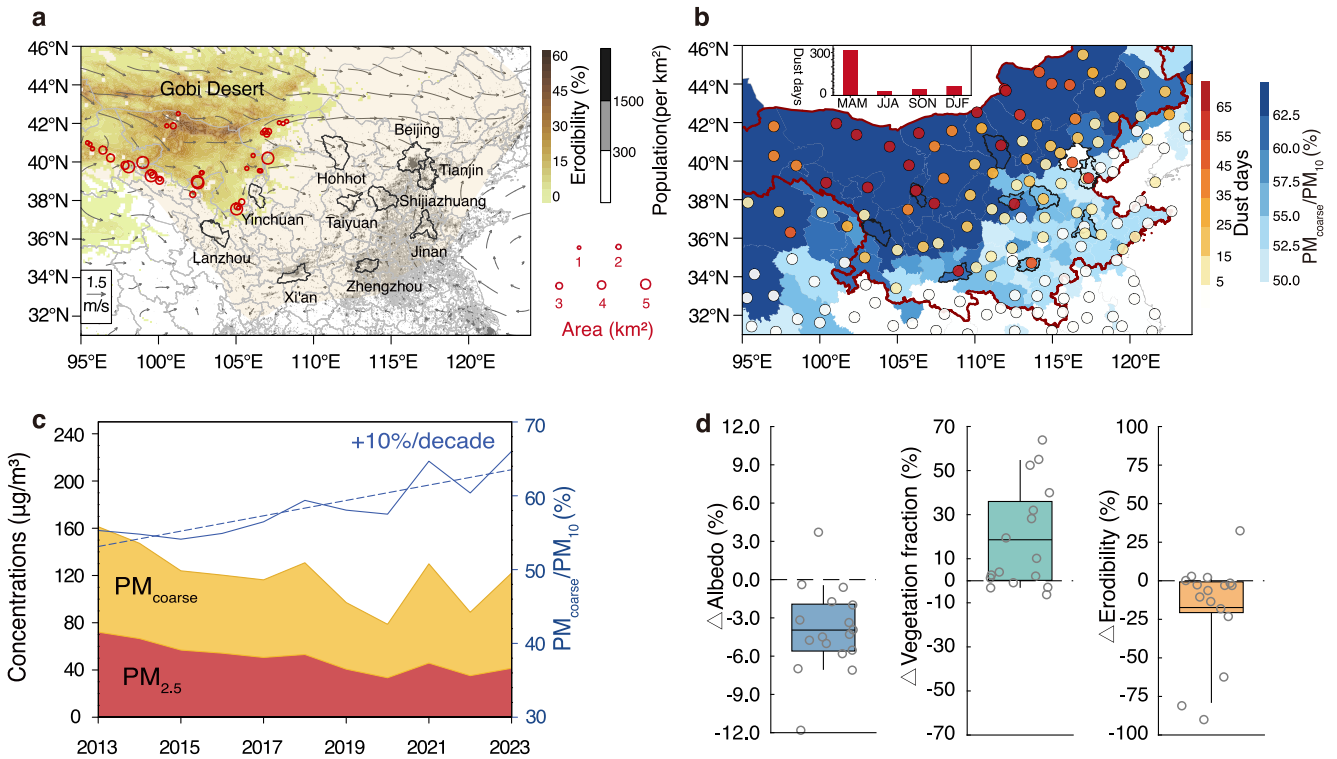


Figure 1. Dust storm pollution in northern China and the impacts of solar farms on surface erodibility. (a) Average springtime soil erodibility (%) during 2013–2023. Red dots, gray arrows, and yellow dots represent solar farms, surface wind vectors, and major dust transport areas, respectively. Representative cities are labeled in black. (b) Springtime (2013–2023) PM_{coarse}/PM_{10} ratio and total dust days. The inset illustrates seasonal dust frequency, and the red boundary outlines the most affected regions. (c) Interannual variation in the $PM_{2.5}$ and PM_{coarse} concentrations, and PM_{coarse}/PM_{10} ratio across the heavily dust-affected cities. (d) Satellite-derived relative changes in springtime surface albedo, vegetation cover, and soil erodibility following solar farm construction. Box plots show the mean as the horizontal line, 25th–75th percentiles as box bounds, and 10th–90th percentiles as whiskers.

Since the launch of China's National Air Quality Action Plan in 2013, $PM_{2.5}$ (particulate matter with diameters less than 2.5 μm) pollution has declined sharply due to reductions in fossil fuel-dominated anthropogenic emissions (Qin et al., 2024) (Figure S3 in Supporting Information S1). Meanwhile, Gobi dust activities show strong interannual variability (Chen et al., 2023; Yin et al., 2022). Consequently, the relative contribution of PM_{coarse} to total PM pollution across dust-affected regions has risen from ~55% in 2013 to ~65% in 2023 (Figure 1c). This shift in pollution characteristics makes natural dust a potential dominant barrier to further urban air-quality improvements, creating an urgent need for innovative, large-scale control solutions and thereby raising the critical scientific question of photovoltaic dust control.

By 2020, a total of 42 solar farms covering an area of over 100 km^2 had been installed across the Gobi Desert, with their spatial distribution largely surrounding the desert (Figure 1a). Satellite observations across 17 representative large solar farms reveal substantial post-construction surface modifications during spring. For the detailed technical descriptions and selection criteria of solar farms, please refer to Text S2 in Supporting Information S1. On average, springtime solar farm deployment reduces surface albedo by 4.0% and increases local vegetation cover by 17.2% relative to the pre-construction baseline, an ecological improvement primarily driven by construction and management practices such as sand fixation and localized irrigation (Wang et al., 2024). This enhanced vegetation subsequently stabilizes the surface and lowers soil erodibility by 17.4% (Figure 1d). Collectively, the composite effects of solar farms, including changes to local radiative, ecological, and soil properties, demonstrate their potential for effective dust mitigation by increasing vegetation cover and lowering soil erodibility, which are less conducive to dust emissions.

19448007, 2026, 17, Downloaded from https://agupubs.onlinelibrary.wiley.com/doi/10.1029/2026GL124605 by Xin Huang - Nanjing University , Wiley Online Library on [17/09/2026]. See the Terms and Conditions (https://onlinelibrary.wiley.com/terms-and-conditions) on Wiley Online Library for rules of use; OA articles are governed by the applicable Creative Commons License

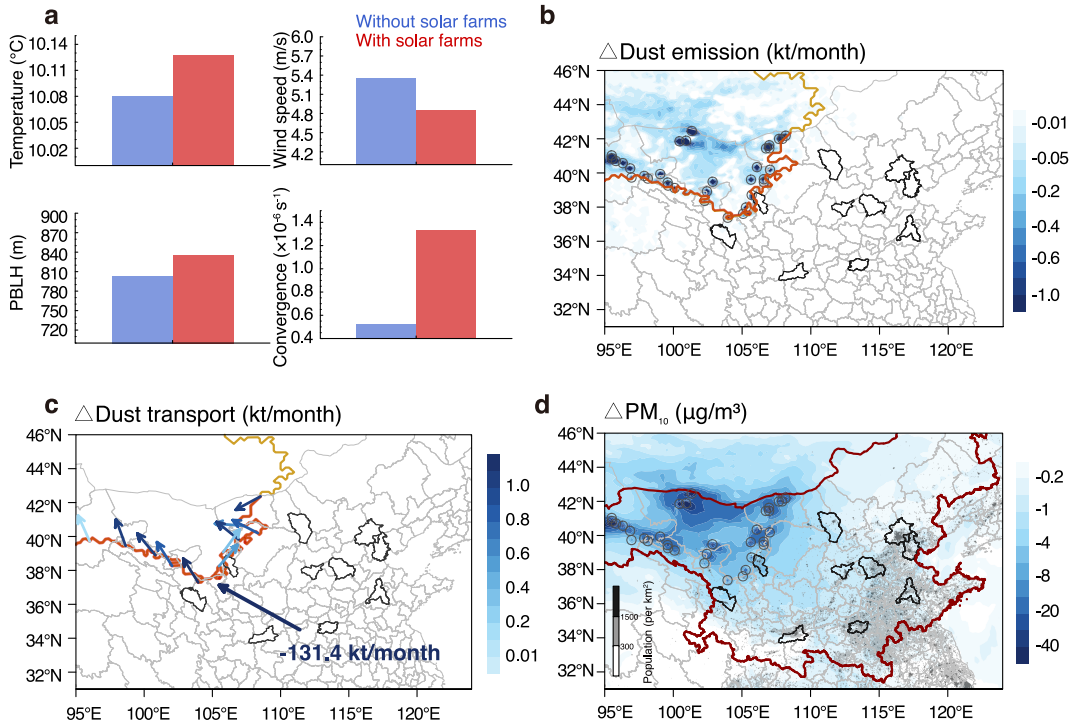


Figure 2. Impacts of solar farms on meteorology, dust emissions, dust transport, and PM_{10} concentrations during spring 2021–2023. (a) Simulated near-surface temperature, 10-m wind speed, boundary layer height, and low-level convergence averaged over solar farms under scenarios with (red) and without (blue) solar farms. (b) Simulated changes in springtime mean dust emission rates, where the yellow and light red outlines denote the Gobi Desert and its Chinese portion, respectively. (c) Spatial distribution of changes in the springtime mean dust transport fluxes, where arrows along the Chinese Gobi boundary reflect the direction and magnitude of flux alterations, with the total absolute change labeled in blue. (d) Changes in springtime near-surface PM_{10} concentrations, with the red boundary outlining the most dust-affected northern Chinese cities.

3.2. Suppressed Dust Pollution by Solar Farm Deployment

Investigating the role of solar farms in regional dust pollution requires air quality models that capture their effects on land surface properties, atmospheric dynamics, and dust emission fluxes. Here, we develop a new solar farm parameterization within the WRF-Chem model. Present-day simulations (spring 2021–2023) validated against observations accurately reproduce regional PM_{10} pollution patterns (Figure S4 in Supporting Information S1). Consistent with satellite observations, the model captures the land surface modifications induced by existing Gobi solar farms, including a 0.04 decrease in albedo, a 1.8% rise in vegetation cover, a 3.1% reduction in soil erodibility, and a 0.07 m increase in roughness length (Figures S5–S6 in Supporting Information S1).

These surface adjustments alter springtime meteorology (Figure 2a and Figure S7 in Supporting Information S1). Increased surface roughness reduces near-surface wind speeds within solar farms by 9.3% (0.5 m/s), primarily due to the physical obstruction of PV arrays that weakens near-surface momentum transport (Jiang et al., 2021). Furthermore, a ∼0.05°C near-surface warming, an average ∼33 m increase in boundary layer height, and a 153.7% (0.8×10^{-6} s^{-1}) intensification of low-level convergence occur above the solar farms, mainly due to PV-reduced surface albedo, which enhances short-wave radiation absorption at the ground surface (Figure 2a).

Combining land surface and meteorological effects, solar farms enhance surface stability and aerodynamic resistance by reducing soil erodibility and near-surface wind speed, decreasing springtime Gobi Desert dust emissions by 352.4 kt/month (Figure 2b). Solar farms situated along the desert margins function analogously to a windbreak wall by attenuating near-surface southward and eastward wind speeds in downwind areas and inducing low-level atmospheric convergence, which subsequently weakens the downstream diffusion of low-altitude dust particles toward major urban centers. Under the combined effects of suppressed emissions and altered meteorology, the total springtime dust transport flux below 1 km into northern China decreases by 131.4 kt/month

19448007, 2026, 17, Downloaded from https://agupubs.onlinelibrary.wiley.com/doi/10.1029/2026GL124605 by Xin Huang - Nanjing University , Wiley Online Library on [17/09/2026]. See the Terms and Conditions (https://onlinelibrary.wiley.com/terms-and-conditions) on Wiley Online Library for rules of use; OA articles are governed by the applicable Creative Commons License

19448007, 2026, 17, Downloaded from https://agupubs.onlinelibrary.wiley.com/doi/10.1029/2026GL124605 by Xin Huang - Nanjing University , Wiley Online Library on [17/09/2026]. See the Terms and Conditions (https://onlinelibrary.wiley.com/terms-and-conditions) on Wiley Online Library for rules of use; OA articles are governed by the applicable Creative Commons License

(Figure 2c). By decoupling these drivers, we estimate that 88% of this transport flux reduction is driven by lower ambient PM_{10} concentrations (i.e., source suppression), while the remaining 12% is attributed to wind field adjustments (i.e., transport attenuation), indicating that downstream PM_{10} mitigation is primarily dominated by the solar farms' source control. Detailed calculations are provided in Texts S4 and S6 in Supporting Information S1. Hence, the dust mitigation effects of solar farms extend across the broader Gobi through long-range transport, ultimately improving urban air quality.

At the current scale of deployment, solar farms already yield measurable reductions in PM_{10} concentrations across northern China (Figure 2d). Cities adjacent to the Gobi Desert (e.g., Yinchuan, Lanzhou, and Hohhot) experience the greatest average springtime PM_{10} reductions of up to 8 $\mu g/m^3$. Importantly, air quality benefits from solar farms depend strongly on pollution severity and are amplified during severe dust events (see Text S7 and Table S4 in Supporting Information S1 for a summary of air quality standards). We estimate that on days with PM_{10} exceeding 250 $\mu g/m^3$—higher than the Chinese National Ambient Air Quality Standards (NAAQS)-Grade V, regional average reductions can reach up to 5.7 $\mu g/m^3$ (4.0–7.5 $\mu g/m^3$, an average 2.0% reduction). On days with lower pollution levels, when PM_{10} concentrations range from 150 to 250 $\mu g/m^3$ (meeting NAAQS-Grade V) and less than 150 $\mu g/m^3$ (meeting World Health Organization (WHO)-Interim Target 1), regional average reductions are 4.2 $\mu g/m^3$ (2.6–4.6 $\mu g/m^3$, an average 2.2% reduction) and 2.3 $\mu g/m^3$ (1.6–2.7 $\mu g/m^3$, an average 2.1% reduction), respectively. This increasing mitigation effectiveness with pollution severity occurs because severe dust events, characterized by strong background winds, simultaneously elevate dust emissions and downwind transport, where the absolute wind-attenuation effects of PV arrays are maximized to subsequently suppress emission and transport fluxes via non-linear scaling (Figure S8 in Supporting Information S1).

3.3. Urban Air Quality Co-Benefits of Solar Farms Expansion Under China's Carbon Neutrality Goal

China's carbon neutrality goals are accelerating the transition toward renewables, with the solar power share in electricity generation projected to rise to 23.3% by 2060 (Qin et al., 2024; Tong et al., 2020), substantially reducing anthropogenic emissions across northern China (Figure 3a and Figure S9a in Supporting Information S1). However, natural dust emissions driven by climate change may threaten these environmental efforts. Future-period (2059–2061) simulations are conducted (see Text S5 in Supporting Information S1 for detailed configuration), and model projections indicate that climate-driven increases in wind speed could elevate springtime Gobi dust emissions by 13.4% and transport fluxes by 27.5% by 2060 (Figure 3b and Figure S9c in Supporting Information S1). Consequently, cities downwind of the Gobi experience springtime PM_{10} increases exceeding 15 $\mu g/m^3$ (Figure S9d in Supporting Information S1), facing approximately 20 heavily-polluted days (daily $PM_{10} > 250$ $\mu g/m^3$) during spring. Across northern China, the regional average PM_{coarse}/PM_{10} ratio is expected to rise from 18.3% to 21.3% due to declining anthropogenic emissions and intensified dust storms. Driven by the sharpest decreases in anthropogenic sources, eastern downwind cities such as Zhengzhou and Jinan exhibit the most pronounced increases in this ratio, as detailed in Figure 3b and Figure S9e in Supporting Information S1. This shifting particulate matter profile underscores the growing necessity of integrating natural dust mitigation into future air quality policies.

Under China's 2060 solar targets, the modeled solar farm area expands to approximately 140,000 km^2, nearly an 11-fold increase over the present-day scenario (Figure 3c, Figure S10 and Text S5 in Supporting Information S1). This future large-scale deployment reduces dust emissions by 12.2% and dust transport by 21.2%, yielding an order-of-magnitude greater mitigation capacity than the current stage and highlighting strong scale-dependent benefits (Figure 3b and Figure S11 in Supporting Information S1). Future large-scale solar farm deployment is expected to effectively reduce PM pollution, with local PM_{10} concentrations in affected urban areas decreasing by more than 100 $\mu g/m^3$, ultimately delivering notable urban air quality improvements (Figure S11 in Supporting Information S1). We further estimate changes in PM_{10} concentrations using both population-weighted (P-W) and area-weighted (A-W) metrics (Text S8 in Supporting Information S1). Future projections show that solar farm deployment could lower average springtime PM_{10} across northern China by 13.7 $\mu g/m^3$ (14.5%) for P-W and 15.9 $\mu g/m^3$ (13.8%) for A-W (Figure 3c; Figure S12 in Supporting Information S1). These relative reductions are 15-fold (P-W) and 13-fold (A-W) greater than the 2021–2023 averages. The greater P-W reduction indicates that large-scale solar farms primarily benefit densely populated metropolitan regions. Furthermore, while the absolute PM_{10} reductions remain concentrated near the Gobi source (up to 100 $\mu g/m^3$), the relative improvements in eastern provinces scale up by 17–18 fold, promoting a more equitable spatial distribution of urban air quality.

10.1029/2026GL124605

19448007, 2026, 17, Downloaded from https://agupubs.onlinelibrary.wiley.com/doi/10.1029/2026GL124605 by Xin Huang - Nanjing University , Wiley Online Library on [17/09/2026]. See the Terms and Conditions (https://onlinelibrary.wiley.com/terms-and-conditions) on Wiley Online Library for rules of use; OA articles are governed by the applicable Creative Commons License

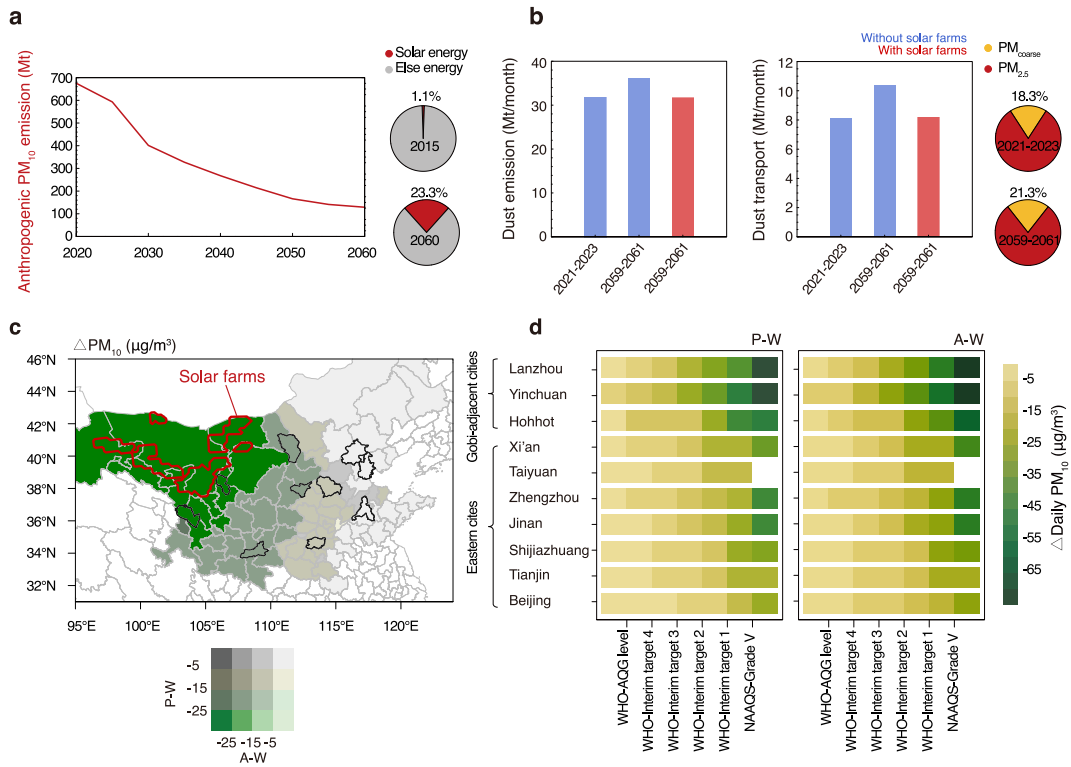


Figure 3. Dust pollution changes and solar power contributions under the carbon neutrality target, and the resulting impact of solar farms on air quality in northern Chinese cities. (a) Springtime anthropogenic PM_{10} emissions from 2020 to 2060. Inset pie charts indicate China's solar power shares in total electricity generation for 2015 and 2060. (b) Springtime dust emissions and transport fluxes (Mt/month) across present-day (2021–2023) and future (2059–2061) periods. Blue and red represent scenarios without and with solar farms, and pie charts show corresponding PM_{coarse}/PM_{10} ratios. (c) Absolute PM_{10} changes due to solar farm construction, represented by area-weighted (A-W) and population-weighted (P-W) PM_{10}. Red border marks the location of solar farms projected under the carbon neutrality target. (d) City-level absolute changes in 2060 springtime P-W (left) and A-W (right) PM_{10} concentrations grouped by air quality conditions, where curly brackets classify cities into Gobi-adjacent and eastern Chinese regions.

Consistent with present-day patterns, solar farms are particularly effective in mitigating PM_{10} concentrations during severe dust events (Figure 3d). Specifically, on days when air quality exceeds NAAQS-Grade V thresholds (daily PM_{10} exceeds 250 μg/m^3), Gobi-adjacent cities experience P-W and A-W reductions of 71.0 μg/m^3 (20.5%) and 71.5 μg/m^3 (21.0%), respectively, compared with more moderate reductions of 35.9 μg/m^3 (10.9%) and 37.0 μg/m^3 (11.2%) across eastern cities (Figure 3d; Figure S12 in Supporting Information S1). Comparatively, on days meeting the strictest standard (WHO-AQG level, daily PM_{10} lower than 45 μg/m^3), PM_{10} reductions are much smaller, with Gobi-adjacent cities showing P-W reductions of 4.6 μg/m^3 (16.5%) and A-W reductions of 4.5 μg/m^3 (16.8%), and eastern cities showing P-W reductions of 1.4 μg/m^3 (5.8%) and A-W reductions of 1.6 μg/m^3 (6.4%). Overall, PV deployment substantially improves air quality, enabling most northern cities to meet the next WHO air quality tier for average springtime daily PM_{10} concentrations, progressing from Interim Target 1 toward the AQG level (Figure S13 in Supporting Information S1), highlighting that carbon-neutral pathways can markedly alleviate air pollution during extreme weather via large-scale PV deployment.

4. Conclusion

By coupling realistic photovoltaic configurations with an interactive dust cycle, our integrated framework explicitly resolves the multi-aspect impacts of solar farms on land-surface properties to demonstrate that solar infrastructure curbs regional dust pollution through synchronized source emission reductions and downwind transport damping. Figure 4 illustrates the underlying atmospheric and ecological mechanisms. Dynamically, panel-induced aerodynamic roughening slows near-surface wind speeds, while associated ecological practices increase vegetation cover and lower surface erodibility, collectively suppressing dust emission at the source.

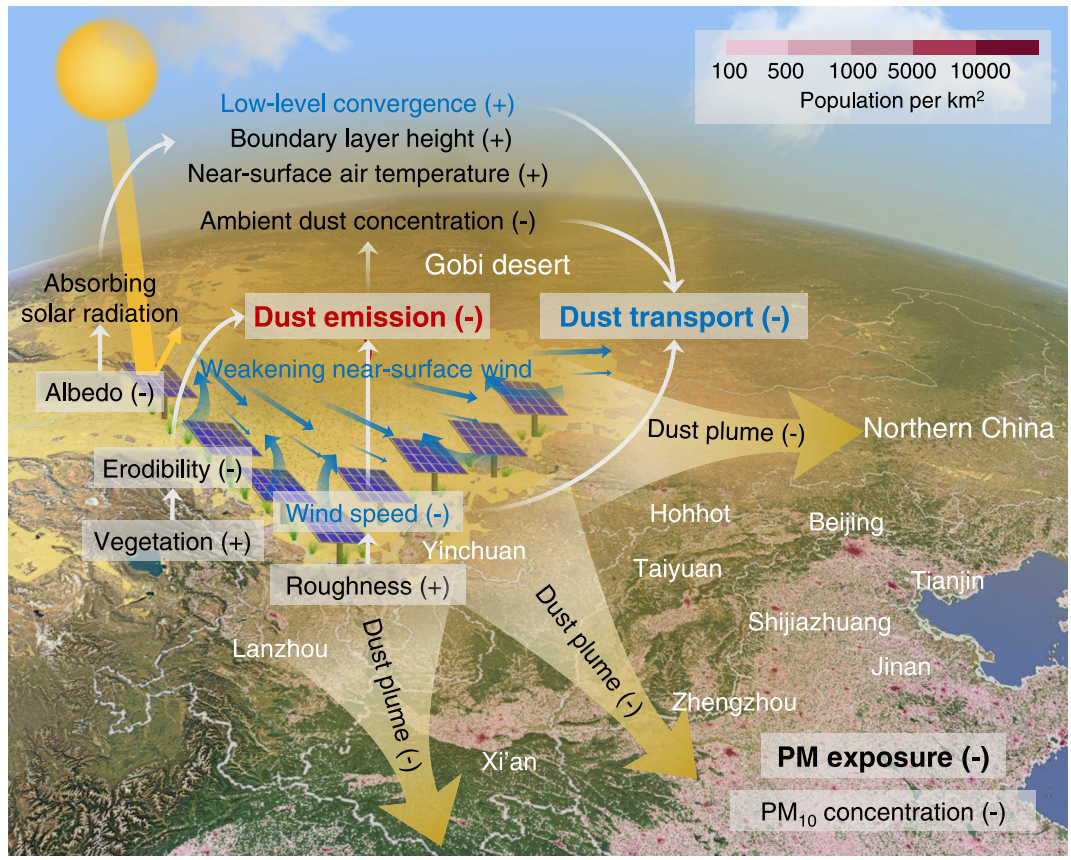


Figure 4. Conceptual scheme of PV-based dust control. Solar farms deployed around the desert margins act to suppress emissions and transport, where positive and negative signs indicate parameter increases and decreases, respectively. Gradient and straight arrows illustrate driving factors, regional wind speed reductions, and altered dust transport pathways from the Gobi Desert toward northern China. The Gobi Desert is marked in yellow, and the 10 most dust-affected provincial-level regions are outlined in white. The locations of representative cities are labeled in white, and the basemap also includes population density (Liu et al., 2024).

Thermally, dark PV arrays reduce surface albedo and enhance solar absorption, warming the near-surface air and deepening the planetary boundary layer. These modifications induce anomalous low-level atmospheric convergence that weakens outflow from the Gobi Desert. Together with lower source emissions, these boundary-layer adjustments collectively curtail downstream dust transport, significantly alleviating particulate matter exposure across northern Chinese cities. Quantitatively, current solar farms reduce springtime regional emissions by 352.4 kt/month and transport by 131.4 kt/month. Under 2060 carbon-neutral expansion, these reductions reach 12.2% and 21.2%, lowering regional PM_{10} by 13.7 μg/m^3 (14.5%) for population-weighted metrics and 15.9 μg/m^3 (13.8%) for area-weighted metrics.

While several simplified assumptions in this pioneering assessment merit further examination (detailed in Text S9 in Supporting Information S1), our findings reveal previously overlooked interconnections between renewable energy and dust dynamics. Ultimately, our findings suggest a paradigm shift in environmental governance—synergizing renewable energy development with ecological restoration—and underscore the importance of strategically planning future solar deployment to maximize dust control co-benefits, particularly in countries facing similar challenges.

Conflict of Interest

The authors declare no conflicts of interest relevant to this study.

19448007, 2026, 17, Downloaded from https://agupubs.onlinelibrary.wiley.com/doi/10.1029/2026GL124605 by Xin Huang - Nanjing University , Wiley Online Library on [17/09/2026]. See the Terms and Conditions (https://onlinelibrary.wiley.com/terms-and-conditions) on Wiley Online Library for rules of use; OA articles are governed by the applicable Creative Commons License

Availability Statement

Information on solar farms is available from Zhang et al. (2022) and Kruitwagen et al. (2021). Albedo data (MCD43A3) are available from Schaaf and Wang (2021), and NDVI (MOD13A1) are from Didan (2021). Snow retrievals (MOD10CM) are from Hall and Riggs (2021). Land cover data (MCD12C1) are available from Friedl and Sulla-Menashe (2022). Terrain heights are obtained from Becker et al. (2009). Dust optical depth and dust records are archived at Voss and Evan (2020) and Smith et al. (2011). Population data of China are available from Jiang et al. (2024) and Liu et al. (2024). Anthropogenic emissions are from the MEIC emission inventory (Li et al., 2017; Zheng et al., 2018) and the DPEC emissions inventory v1.1 (Cheng et al., 2021, 2023; Qin et al., 2024; Tong et al., 2020). ERA5 reanalysis data are available from Hersbach et al. (2023). Meteorological data for 2059–2061 are available at Xu et al. (2021). The source code of the modified WRF-Chem model and the GOCART code, solar-farm run configuration, and erodibility data sets can be downloaded from Hao (2026).

Acknowledgments
This work was supported by the National Natural Science Foundation of China (42588101 and 42325506), the National Key Research and Development Program of China (2024YFC3713401), the Fundamental Research Funds for the Central Universities (14380198), and the New Cornerstone Science Foundation through the XPLORER PRIZE. We are grateful to the High-Performance Computing & Massive Data Center of Nanjing University for running the model on its Blade cluster system.

References

Becker, J. J., Sandwell, D. T., Smith, W. H. F., Braud, J., Binder, B., Depner, J. L., et al. (2009). Global bathymetry and elevation data at 30 arc seconds resolution: SRTM30_PLUS. *Marine Geodesy*, *32*(4), 355–371. https://doi.org/10.1080/01490410903297766

Chang, R., Yan, Y., Wu, J., Wang, Y., & Gao, X. (2023). Projected PV plants in China's gobi deserts would result in lower evaporation and wind. *Solar Energy*, *256*, 140–150. https://doi.org/10.1016/j.solener.2023.04.003

Chang, Z., Liu, S., Fu, J., Wang, Q., Wang, F., Sun, T., et al. (2020). Effect of desert photovoltaic on sand prevention and control—taking Gansu Gulang Zhenfa photovoltaic DC field as an example. *IOP Conference Series: Earth and Environmental Science*, *601*(1), 012032. https://doi.org/10.1088/1755-1315/601/1/012032

Chen, S., Wang, Y., Lu, X., He, K., & Hao, J. (2025). Global disparity in synergy of solar power and vegetation growth. *Environmental Research Letters*, *20*(1), 014066. https://doi.org/10.1088/1748-9326/ada302

Chen, S., Zhao, D., Huang, J., He, J., Chen, Y., Chen, J., et al. (2023). Mongolia contributed more than 42% of the dust concentrations in northern China in march and April 2023. *Advances in Atmospheric Sciences*, *40*(9), 1549–1557. https://doi.org/10.1007/s00376-023-3062-1

Cheng, J., Tong, D., Liu, Y., Geng, G., Davis, S. J., He, K., & Zhang, Q. (2023). A synergistic approach to air pollution control and carbon neutrality in China can avoid millions of premature deaths annually by 2060. *One Earth*, *6*(8), 978–989. https://doi.org/10.1016/j.oneear.2023.07.007

Cheng, J., Tong, D., Zhang, Q., Liu, Y., Lei, Y., Yan, G., et al. (2021). Pathways of China's PM2.5 air quality 2015–2060 in the context of carbon neutrality. *National Science Review*, *8*(12), nwab078. https://doi.org/10.1093/nsr/nwab078

China Daily. (2023). Solar, wind projects to accelerate. Retrieved from https://english.www.gov.cn/statecouncil/ministries/202302/21/content_WS63f41dafc6d0a757729e6fc7.html

Didan, K. (2021). MODIS/terra vegetation indices 16-Day L3 global 500m SIN grid V061. https://doi.org/10.5067/MODIS/MOD13A1.061

Friedl, M., & Sulla-Menashe, D. (2022). MODIS/Terra+ aqua land cover type yearly L3 global 0.05 deg CMG V061. *NASA EOSDIS Land Processes DAAC*. https://doi.org/10.5067/MODIS/MCD12C1 *61*.

Geng, G., Liu, Y., Liu, Y., Liu, S., Cheng, J., Yan, L., et al. (2024). Efficacy of China's clean air actions to tackle PM2.5 pollution between 2013 and 2020. *Nature Geoscience*, *17*(10), 987–994. https://doi.org/10.1038/s41561-024-01540-z

Gutman, G., & Ignatov, A. (1998). The derivation of the green vegetation fraction from NOAA/AVHRR data for use in numerical weather prediction models. *International Journal of Remote Sensing*, *19*(8), 1533–1543. https://doi.org/10.1080/014311698215333

Hall, D. K., & Riggs, G. A. (2021). *MODIS/terra snow cover monthly L3 global 0.05Deg CMG, version 61*. NASA National Snow and Ice Data Center Distributed Active Archive Center. https://doi.org/10.5067/MODIS/MOD10CM.061

Hao, Y. (2026). A modified WRF-chem (v4.4.1) GOCART model and soil erodibility dataset integrating solar photovoltaic station parameterization. *Zenodo*. [Dataset]. https://doi.org/10.5281/zenodo.21339815

Hao, Y., Wang, Z., Xue, L., Lou, S., Ding, K., Qin, Y., & Huang, X. (2024). Modeling the effects of vegetation and snow on dust storm over the gobi desert. *Journal of Geophysical Research: Atmospheres*, *129*(22), e2024JD041407. https://doi.org/10.1029/2024JD041407

Hersbach, H., Bell, B., Berrisford, P., Biavati, G., Horányi, A., Muñoz Sabater, J., et al. (2023). ERA5 hourly data on single levels from 1940 to present. https://doi.org/10.24381/cds.adbb2d47

Hu, A., Levis, S., Meehl, G., Han, W., Washington, W., Oleson, K., et al. (2015). Impact of solar panels on global climate. *Nature Climate Change*, *6*(3), 290–294. https://doi.org/10.1038/nclimate2843

Jiang, C., Liu, J., Zhang, H., Zhang, Z., & Wang, D. (2019). China's progress towards sustainable land degradation control: Insights from the northwest arid regions. *Ecological Engineering*, *127*, 75–87. https://doi.org/10.1016/j.ecoleng.2018.11.014

Jiang, J., Gao, X., & Chen, B. (2021). The impact of utility-scale photovoltaics plant on near surface turbulence characteristics in gobi areas. *Atmosphere*, *12*(1), 18. https://doi.org/10.3390/atmos12010018

Jiang, T., Su, B., Jing, C., Wang, Y., Huang, J., Guo, H., et al. (2024). National and provincial population and economy projection databases under shared socioeconomic pathways (SSP1-5)_v2. *Science Data Bank*. [Dataset]. https://doi.org/10.57760/sciencedb.01683

Kok, J., Storelvmo, T., Karydis, V., Adebiyi, A., Mahowald, N., Evan, A., et al. (2023). Mineral dust aerosol impacts on global climate and climate change. *Nature Reviews Earth & Environment*, *4*(2), 71–86. https://doi.org/10.1038/s43017-022-00379-5

Kruitwagen, L., Story, K. T., Friedrich, J., Byers, L., Skillman, S., & Hepburn, C. (2021). A global inventory of photovoltaic solar energy generating units. *Nature*, *598*(7882), 604–610. https://doi.org/10.1038/s41586-021-03957-7

Li, M., Liu, H., Geng, G., Hong, C., Liu, F., Song, Y., et al. (2017). Anthropogenic emission inventories in China: A review. *National Science Review*, *4*(6), 834–866. https://doi.org/10.1093/nsr/nwx150

Li, X., He, Z., Xia, S., & Yang, Y. (2024). Greenness change associated with construction and operation of photovoltaic solar energy in China. *Renewable Energy*, *226*, 120461. https://doi.org/10.1016/j.renene.2024.120461

Li, Y., Kalnay, E., Motesharrei, S., Rivas, J., Kucharski, F., Kirk-Davidoff, D., et al. (2018). Climate model shows large-scale wind and solar farms in the Sahara increase rain and vegetation. *Science*, *361*(6406), 1019–1022. https://doi.org/10.1126/science.aar5629

Li, Y., Wang, Z., Lei, Y., Yu, X., Chen, F., Wang, Z., et al. (2025). Satellite-based climate effects of photovoltaic plants in China. *Journal of Geophysical Research: Atmospheres*, *130*(11), e2025JD044085. https://doi.org/10.1029/2025JD044085

19448007, 2026, 17, Downloaded from https://agupubs.onlinelibrary.wiley.com/doi/10.1029/2026GL124605 by Xin Huang - Nanjing University , Wiley Online Library on [17/09/2026]. See the Terms and Conditions (https://onlinelibrary.wiley.com/terms-and-conditions) on Wiley Online Library for rules of use; OA articles are governed by the applicable Creative Commons License

Liu, L., Cao, X., Li, S., & Jie, N. (2024). A 31-year (1990–2020) global gridded population dataset generated by cluster analysis and statistical learning. *Scientific Data*, *11*(1), 124. https://doi.org/10.1038/s41597-024-02913-0

Long, J., Lu, Z., Miller, P. A., Pongratz, J., Guan, D., Smith, B., et al. (2024). Large-scale photovoltaic solar farms in the Sahara affect solar power generation potential globally. *Communications Earth & Environment*, *5*(1), 1–9. https://doi.org/10.1038/s43247-023-01117-5

Lu, X., Chen, S., Nielsen, C. P., Zhang, C., Li, J., Xu, H., et al. (2021). Combined solar power and storage as cost-competitive and grid-compatible supply for China's future carbon-neutral electricity system. *Proceedings of the National Academy of Sciences*, *118*(42), e2103471118. https://doi.org/10.1073/pnas.2103471118

Min, Q.-L., Li, R., Lin, B., Joseph, E., Wang, S., Hu, Y., et al. (2009). Evidence of mineral dust altering cloud microphysics and precipitation. *Atmospheric Chemistry and Physics*, *9*(9), 3223–3231. https://doi.org/10.5194/acp-9-3223-2009

Nguyen, K., Katzfey, J., Riedl, J., & Troccoli, A. (2017). Potential impacts of solar arrays on regional climate and on array efficiency: Potential impacts of solar arrays on regional climate. *International Journal of Climatology*, *37*(11), 4053–4064. https://doi.org/10.1002/joc.4995

Power, K., Lu, Z., & Zhang, Q. (2023). Impacts of large-scale Saharan solar farms on the global terrestrial carbon cycle. *Environmental Research Letters*, *18*(10), 104009. https://doi.org/10.1088/1748-9326/acf7d8

Qin, Y., Zhou, M., Hao, Y., Huang, X., Tong, D., Huang, L., et al. (2024). Amplified positive effects on air quality, health, and renewable energy under China's carbon neutral target. *Nature Geoscience*, *17*(5), 411–418. https://doi.org/10.1038/s41561-024-01425-1

Schaaf, C., & Wang, Z. (2021). MODIS/Terra+Aqua BRDF/Albedo daily L3 global - 500m V061. https://doi.org/10.5067/MODIS/MCD43A3.061

Smith, A., Lott, N., & Vose, R. (2011). The integrated surface database: Recent developments and partnerships. *Bulletin of the American Meteorological Society*, *92*(6), 704–708. https://doi.org/10.1175/2011bams3015.1

Stern, R., Müller, J., Rotenberg, E., Amer, M., Segev, L., & Yakir, D. (2023). Photovoltaic fields largely outperform afforestation efficiency in global climate change mitigation strategies. *PNAS Nexus*, *2*(11), pgad352. https://doi.org/10.1093/pnasnexus/pgad352

Tan, M., & Li, X. (2015). Does the green great Wall effectively decrease dust storm intensity in China? A study based on NOAA NDVI and weather station data. *Land Use Policy*, *43*, 42–47. https://doi.org/10.1016/j.landusepol.2014.10.017

Tong, D., Cheng, J., Liu, Y., Yu, S., Yan, L., Hong, C., et al. (2020). Dynamic projection of anthropogenic emissions in China: Methodology and 2015–2050 emission pathways under a range of socio-economic, climate policy, and pollution control scenarios. *Atmospheric Chemistry and Physics*, *20*(9), 5729–5757. https://doi.org/10.5194/acp-20-5729-2020

Voss, K. K., & Evan, A. T. (2020). A new satellite-based global climatology of dust aerosol optical depth. *Journal of Applied Meteorology and Climatology*, *59*(1), 83–102. https://doi.org/10.1175/JAMC-D-19-0194.1

Wang, Y., Liu, B., Xing, Y., Peng, H., Wu, H., & Zhong, J. (2024). Ecological construction status of photovoltaic power plants in China's deserts. *Frontiers in Environmental Science*, *12*, 1406546. https://doi.org/10.3389/fenvs.2024.1406546

Wei, S., Ziegler, A. D., Qin, Y., Wang, D., Chen, Y., Yan, J., & Zeng, Z. (2024). Small reduction in land surface albedo due to solar panel expansion worldwide. *Communications Earth & Environment*, *5*(1), 1–10. https://doi.org/10.1038/s43247-024-01619-w

Wu, C., Lin, Z., Shao, Y., Liu, X., & Li, Y. (2022). Drivers of recent decline in dust activity over East Asia. *Nature Communications*, *13*(1), 7105. https://doi.org/10.1038/s41467-022-34823-3

Xia, Z., Li, Y., Zhang, W., Guo, S., Zheng, L., Jia, N., et al. (2023). Quantitatively distinguishing the impact of solar photovoltaics programs on vegetation in dryland using satellite imagery. *Land Degradation & Development*, *34*(14), 4373–4385. https://doi.org/10.1002/ldr.4783

Xu, Z., Han, Y., Tam, C.-Y., Yang, Z.-L., & Fu, C. (2021). Bias-corrected CMIP6 global dataset for dynamical downscaling of the historical and future climate (1979–2100). *Scientific Data*, *8*(1), 293. https://doi.org/10.1038/s41597-021-01079-3

Xu, Z., Li, Y., Qin, Y., & Bach, E. (2024). A global assessment of the effects of solar farms on albedo, vegetation, and land surface temperature using remote sensing. *Solar Energy*, *268*, 112198. https://doi.org/10.1016/j.solener.2023.112198

Yang, A., Tan, Q., Rajapakshe, C., Chin, M., & Yu, H. (2022). Global premature mortality by dust and pollution PM2.5 estimated from aerosol reanalysis of the modern-era retrospective analysis for research and applications, version 2. *Frontiers in Environmental Science*, *10*, 975755. https://doi.org/10.3389/fenvs.2022.975755

Yang, Y., Russell, L. M., Lou, S., Liao, H., Guo, J., Liu, Y., et al. (2017). Dust-wind interactions can intensify aerosol pollution over eastern China. *Nature Communications*, *8*(1), 15333. https://doi.org/10.1038/ncomms15333

Yin, Z., Wan, Y., Zhang, Y., & Wang, H. (2022). Why super sandstorm 2021 in North China? *National Science Review*, *9*(3), nwab165. https://doi.org/10.1093/nsr/nwab165

Zhang, C., Yan, M., Du, H., Ban, J., Chen, C., Liu, Y., & Li, T. (2023). Mortality risks from a spectrum of causes associated with sand and dust storms in China. *Nature Communications*, *14*(1), 6867. https://doi.org/10.1038/s41467-023-42530-w

Zhang, X., & Xu, M. (2020). Assessing the effects of photovoltaic powerplants on surface temperature using remote sensing techniques. *Remote Sensing*, *12*(11), 1825. https://doi.org/10.3390/rs12111825

Zhang, X., Xu, M., Wang, S., Huang, Y., & Xie, Z. (2022). Mapping photovoltaic power plants in China using landsat, random forest, and Google Earth Engine. *Earth System Science Data*, *14*(8), 3743–3755. https://doi.org/10.5194/essd-14-3743-2022

Zhao, D., Chen, H., Yu, E., & Luo, T. (2019). PM2.5/PM10 ratios in eight economic regions and their relationship with meteorology in China. *Advances in Meteorology*, *2019*(1), 5295726. https://doi.org/10.1155/2019/5295726

Zheng, B., Tong, D., Li, M., Liu, F., Hong, C., Geng, G., et al. (2018). Trends in China's anthropogenic emissions since 2010 as the consequence of clean air actions. *Atmospheric Chemistry and Physics*, *18*(19), 14095–14111. https://doi.org/10.5194/acp-18-14095-2018

References From the Supporting Information

Bao, J., Li, X., Yu, T., Jiang, L., Zhang, J., Song, F., & Xu, W. (2024). Are regions conducive to photovoltaic power generation demonstrating significant potential for harnessing solar energy via photovoltaic systems? *Sustainability*, *16*(8), 3281. https://doi.org/10.3390/su16083281

Chang, X., Wang, S., Zhao, B., Cai, S., & Hao, J. (2018). Assessment of inter-city transport of particulate matter in the Beijing–Tianjin–Hebei region. *Atmospheric Chemistry and Physics*, *18*(7), 4843–4858. https://doi.org/10.5194/acp-18-4843-2018

Chen, S., Lu, X., Miao, Y., Deng, Y., Nielsen, C. P., Elbot, N., et al. (2019). The potential of photovoltaics to power the belt and road initiative. *Joule*, *3*(8), 1895–1912. https://doi.org/10.1016/j.joule.2019.06.006

Chen, S., Lu, X., Nielsen, C. P., Geng, G., He, K., McElroy, M. B., et al. (2022). Improved air quality in China can enhance solar-power performance and accelerate carbon-neutrality targets. *One Earth*, *5*(5), 550–562. https://doi.org/10.1016/j.oneear.2022.04.002

Guo, X., Dong, Y., & Ren, D. (2023). CO2 emission reduction effect of photovoltaic industry through 2060 in China. *Energy*, *269*, 126692. https://doi.org/10.1016/j.energy.2023.126692

19448007, 2026, 17, Downloaded from https://agupubs.onlinelibrary.wiley.com/doi/10.1029/2026GL124605 by Xin Huang - Nanjing University , Wiley Online Library on [17/09/2026]. See the Terms and Conditions (https://onlinelibrary.wiley.com/terms-and-conditions) on Wiley Online Library for rules of use; OA articles are governed by the applicable Creative Commons License

He, G., & Kammen, D. M. (2016). Where, when and how much solar is available? A provincial-scale solar resource assessment for China. *Renewable Energy*, *85*, 74–82. https://doi.org/10.1016/j.renene.2015.06.027

He, G., Lin, J., Sifuentes, F., Liu, X., Abhyankar, N., & Phadke, A. (2020). Rapid cost decrease of renewables and storage accelerates the decarbonization of China's power system. *Nature Communications*, *11*(1), 2486. https://doi.org/10.1038/s41467-020-16184-x

Li, Y., Zhao, M., Motesharrei, S., Mu, Q., Kalnay, E., & Li, S. (2015). Local cooling and warming effects of forests based on satellite observations. *Nature Communications*, *6*(1), 6603. https://doi.org/10.1038/ncomms7603

Liu, Y., Tang, G., Zhou, L., Hu, B., Liu, B., Li, Y., et al. (2019). Mixing layer transport flux of particulate matter in Beijing, China. *Atmospheric Chemistry and Physics*, *19*(14), 9531–9540. https://doi.org/10.5194/acp-19-9531-2019

Lu, Z., Zhang, Q., Miller, P. A., Zhang, Q., Berntell, E., & Smith, B. (2021). Impacts of large-scale sahara solar farms on global climate and vegetation cover. *Geophysical Research Letters*, *48*(2), e2020GL090789. https://doi.org/10.1029/2020GL090789

Lyu, X., Li, X., Zhang, C., Dang, D., Wang, K., & Lou, A. (2024). Mapping the carbon mitigation potential of photovoltaic development in the Gobi and desert regions of China. *Energy*, *308*, 132936. https://doi.org/10.1016/j.energy.2024.132936

Ministry of Ecology and Environment of the People's Republic of China. (2013). Technical regulation for ambient air quality assessment (on trial) (HJ 663-2013). Retrieved from https://www.chinesestandard.net/PDF-EN/HJ633-2012EN-P07P-H5843H-654914.pdf

Millstein, D., & Menon, S. (2011). Regional climate consequences of large-scale cool roof and photovoltaic array deployment. *Environmental Research Letters*, *6*(3), 034001. https://doi.org/10.1088/1748-9326/6/3/034001

Tang, W., Xu, S., Zhou, X., Yang, K., Wang, Y., Qin, J., et al. (2023). Meeting China's electricity demand with renewable energy over Tibetan Plateau. *Science Bulletin*, *68*(1), 39–42. https://doi.org/10.1016/j.scib.2022.12.012

Ukhov, A., Ahmadov, R., Grell, G., & Stenchikov, G. (2021). Improving dust simulations in WRF-chem v4.1.3 coupled with the GOCART aerosol module. *Geoscientific Model Development*, *14*(1), 473–493. https://doi.org/10.5194/gmd-14-473-2021

UNEP-WCMC and IUCN. (2025). Protected planet: The world database on protected areas (WDPA). https://doi.org/10.34892/6fwd-af11

Wang, S., Lü, L., Zhang, B., Wang, S., Wu, J., Fu, J., & Luo, H. (2021). Multi-objective programming model of low-cost path for China's peaking carbon dioxide emissions and carbon neutrality. *Research of Environmental Sciences*, *34*(9), 2044–2055. https://doi.org/10.13198/j.issn.1001-6929.2021.06.18

Wang, Y., Lin, R., Liu, C., Wang, X., Chosy, C., Haruta, Y., et al. (2024). Homogenized contact in all-perovskite tandems using tailored 2D perovskite. *Nature*, *635*(8040), 867–873. https://doi.org/10.1038/s41586-024-08158-6

World Health Organization. (2021). *WHO global air quality guidelines: Particulate matter (PM2.5 and PM10), ozone, nitrogen dioxide, sulfur dioxide and carbon monoxide*. World Health Organization.

Xia, Z., Li, Y., Guo, S., Chen, R., Zhang, W., Guo, X., et al. (2024). Satellites reveal spatial heterogeneity in dryland photovoltaic plants' effects on vegetation dynamics. *Earth's Future*, *12*(6), e2024EF004427. https://doi.org/10.1029/2024EF004427

Zhang, D., Zhu, Z., Chen, S., Zhang, C., Lu, X., Zhang, X., et al. (2024). Spatially resolved land and grid model of carbon neutrality in China. *Proceedings of the National Academy of Sciences*, *121*(10), e2306517121. https://doi.org/10.1073/pnas.2306517121

Zhu, W.-K., Wang, C., Wang, L., Wu, X., & Yue, Q. (2022). Analysis of energy-saving and environmental benefits from power structure adjustment in China: A comparative study from 2020 to 2060. *Sustainable Production and Consumption*, *31*, 750–761. https://doi.org/10.1016/j.spc.2022.03.030

19448007, 2026, 17, Downloaded from https://agupubs.onlinelibrary.wiley.com/doi/10.1029/2026GL124605 by Xin Huang - Nanjing University , Wiley Online Library on [17/09/2026]. See the Terms and Conditions (https://onlinelibrary.wiley.com/terms-and-conditions) on Wiley Online Library for rules of use; OA articles are governed by the applicable Creative Commons License